

Synthesis and characterization of SnO₂-Mn₂O₃ Nano composite materials

B. Linga Reddy

Chaitanya Bharati Institute of Technology, Hyderabad, India 500075

Abstract:

A novel green approach has been adopted for the preparation of SnO₂-Mn₂O₃ nano composite material avoiding the use of harmful organic precursors, solvents, capping ligands and templates which is the prime advantage of the green synthetic approach. The nano composites obtained were analyzed by low angle, wide angle X-ray diffraction, surface area by BET and scanning electron microscopy (SEM)

1. Introduction

In the recent times, considerable developments in the preparation of well ordered mesoporous materials have triggered research efforts in catalysis, catalysis supports and adsorbents because of their high-specific surface areas, large specific pore volumes, and narrow pore size distribution^{1(a-g)}. Crystalline nanomaterials consisting of complex metal or metal oxides are generally known as nanocomposites. Metal or metal oxide nanoparticles or their nanocomposites are usually synthesized by electrochemical deposition or chemical deposition methods followed by decomposition or reduction in the confined channels of host materials such as carbon nanotubes^{2(a-b)}, anodic aluminum membranes³, and micro porous or mesoporous molecular sieves^{4(a-c)}.

In the traditional strategy, such as wetness impregnation or ion exchange, metal salt diffuses easily to the outer surface of the host silica to form large metal aggregates during the reduction or thermal treatment process.^{5(a-c)} To overcome this disadvantage, Chao et al. functionalized the intrachannel surface of the host silica and then fabricated highly dispersed a new in-situ reduction to produce the Pd nanocoating in the channels of selectively modified mesoporous silica SBA-15^{6(a-b)}. At this juncture, formation of metastable solid solution^{7(a-b)} or introduction of second phase is an indispensable requirement to prevent the particle growth or sintering of nanoparticles.

By using the second metal and without using harmful organic precursors, solvents, templates and capping agents, SnO₂ – Mn₂O₃ binary mixed metal oxide

nanocomposites are prepared by adjusting synthetic variables of conventional co-precipitation technique using eco-friendly chemicals and conditions. The deposition of SnO₂ – Mn₂O₃ nanocomposites on the mesoporous SBA-15 has been delineated.

2. Experimental procedure:

2.1 Preparation of Mn₂O₃-SnO₂-SBA-15

Dispersion of nano composites on hexagonally ordered mesoporous SBA-15 has been achieved by precipitation-deposition method taking the requisite amount of homogeneous mixed salt solution of Sn and Mn with high dilution at room temperature under constant stirring.. The requisite amount of SBA-15 dispersed in the mixed salt solution. Subsequently diluted aqueous ammonium solution added under stirring. Precipitation of mixed salt solution and its deposition on the surface of hexagonally ordered mesoporous SBA-15 material takes place simultaneously. The p123 template was removed by calcination in static air. Finally the powdered mesonano composite material was separated by a simple filtration and dried at 110 °C in air oven for 12 h followed by conducted the calcinations at 500 °C for 6 h. The calcinated Mn₂O₃-SnO₂-SBA-15 meso-nano composite materials were characterized by low angle XRD, wide angle XRD, nitrogen adsorption-dispersion and SEM techniques.

2.2. Characterization by X-Ray Diffraction:

XRD patterns of nanocomposites were recorded by a Rigaku Miniflex X-ray diffractometer (M/S.Rigaku Corporation, Japan) using Ni filtered Cu K_α radiation with scan speed 2°min⁻¹ and 2θ range from 10-80°.The low angle XRD patterns were obtained from Altima –IV Rigaku X-ray diffractometer (M/S. Rigaku Corporation, Japan) using Ni filtered Cu K_α radiation with scan 1°min⁻¹ and 2θ range from 0.7-5°.

2.3. Characterization by BET Surface Area

Surface area was determined by BET single point method, single point measurements are accomplished using a 30% N₂ /70% He gas mixture.The sample was pre-heated to remove all moisture in flow of pure He (99.99 %) at 473 K for 2 h.After the completion of pretreatment N₂ through the sample tube, which is placed in a liquid N₂ bath (77 K).

2.4. Characterization by Scanning Electron Microscopy

The scanning electron microscopy (SEM) images and energy-dispersed X-ray spectrometer (EDX) were taken on a Hitachi S-800 field-emission scanning electron microscope and S-2400 scanning electron microscope, respectively.

3. Results and discussion:

3.1 Characterization of Mn₂O₃-SnO₂-SBA-15 by low angle XRD

In the low angle region of XRD (Fig-1) the calcinated SBA-15 exhibits intense diffraction peaks, characteristic of a two –dimensional hexagonal (p6mm) structure

with d_{100} spacing of ca. 98.9 \AA . After $\text{Mn}_2\text{O}_3\text{-SnO}_2$ nanocomposite deposition, the overall pore structure was retained, indicated by the appearance of high ordered reflection peaks of the sample. However, the XRD pattern of $\text{Mn}_2\text{O}_3\text{-SnO}_2\text{-SBA-15}$ composite shows the decrease in peak intensity, especially for (110) and (200) reflections. This is probably due to the difference on the scattering contrasts of the pore and the walls, and to the formation of nono structured $\text{Mn}_2\text{O}_3\text{-SnO}_2$ inside the channels of SBA-15 as in the case of MCM-41⁸

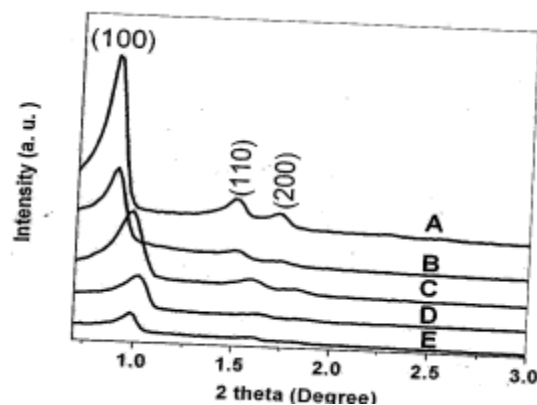


Fig-1: Low angle XRD of $\text{Mn}_2\text{O}_3\text{-SnO}_2\text{-SBA-15}$ meso-nanocomposite materials (A) SAB-15, (B) 10% $\text{Mn}_1\text{Sn}_9\text{/SAB-15}$, (C) 15% $\text{Mn}_1\text{Sn}_9\text{/SAB-15}$ (D) 20% $\text{Mn}_1\text{Sn}_9\text{/SAB-15}$ (E) 25% $\text{Mn}_1\text{Sn}_9\text{/SAB-15}$

3.2 Characterization of $\text{Mn}_2\text{O}_3\text{-SnO}_2\text{-SBA-15}$ by wide- angle XRD

In the wide- angle region of XRD, $\text{Mn}_2\text{O}_3\text{-SnO}_2\text{-SBA-15}$ exhibits four distinct peaks contributed by SnO_2 metal oxide (Fig-2). These peaks are very broad and weak, indicating the nanocrystalline nature of SnO_2 in the composite. It also suggests that no large SnO_2 particles would give intense and sharp diffraction signals and dominated the resulting diffraction pattern of the composite. The advantage Pt particle size was estimated to be $\leq 5 \text{ nm}$, from the peak width of SnO_2 (101) reflection by using Scherrer's equation with a spherical model for approximation.

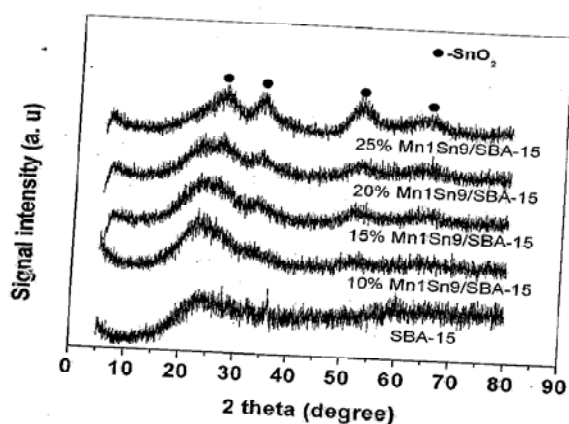


Fig-2: Wide-angle XRD of $\text{Mn}_2\text{O}_3\text{-SnO}_2\text{-SBA-15}$ meso-nanocomposite materials

3.3 Characterization of $\text{Mn}_2\text{O}_3\text{-SnO}_2\text{-SBA-15}$ by N_2 Adsorption

Nitrogen adsorption-desorption isotherm for calcined SBA-15 and nanocomposite incorporated ($\text{Mn}_2\text{O}_3\text{-SnO}_2\text{-SBA-15}$) are shown in Fig-3. The isotherms feature hysteresis loops with sharp adsorption and desorption branches in at $p/p_0=0.69$, indicating a narrow mesopore size distribution.

After $\text{Mn}_2\text{O}_3\text{-SnO}_2$ incorporation, the total pore volume and mesopore volume decreased with a slight decrease of the average size. This suggests that most of the nanometer-scaled void space of SBA-15 silica is open, although a small portion of the channels may be stuck by the $\text{Mn}_2\text{O}_3\text{-SnO}_2$ nanoparticles.

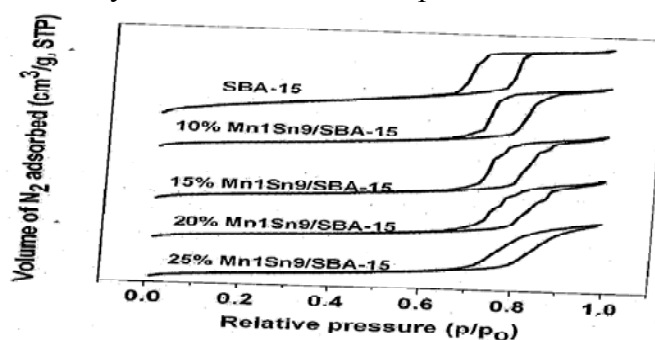


Fig-3: Adsorption- desorption isotherms of $\text{Mn}_2\text{O}_3\text{-SnO}_2\text{-SBA-15}$ meso-nanocomposite materials

3.4 Characterization of $\text{Mn}_2\text{O}_3\text{-SnO}_2\text{-SBA-15}$ by N_2SEM

Scanning electron microscopic image of $\text{Mn}_2\text{O}_3\text{-SnO}_2\text{-SBA-15}$ has been displayed in Fig -4, from which, the morphology of $\text{Mn}_2\text{O}_3\text{-SnO}_2\text{-SBA-15}$ is more or less similar to calcinated SBA-15.i.e.fiber like morphology. However, the morphology certain extent disturbed due to incorporation of $\text{Mn}_2\text{O}_3\text{-SnO}_2$.

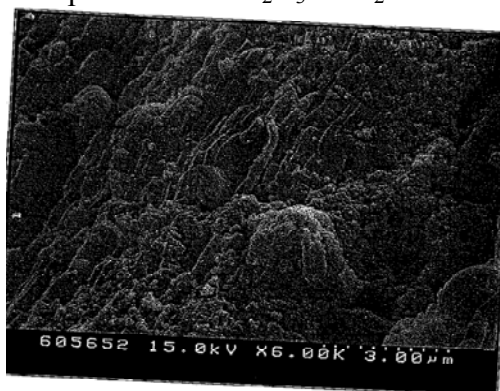


Fig-4: SEM image of $\text{Mn}_2\text{O}_3\text{-SnO}_2\text{-SBA-15}$ Meso-nanocomposite materials

4. Conclusion:

Synthesis of new $\text{Mn}_2\text{O}_3\text{-SnO}_2\text{-SBA-15}$ mesonanocomposite materials has successfully been achieved by a green synthetic approach (GSA), wherein; traditionally used environmentally harmful organic solvents; organic metal precursors

and organic ligands are avoided in the possible extent. The usage of diluted ammonia precipitation agent and highly diluted Sn, Mn, Zr, Ce salt precursors are critical for the formation of nanocomposites. Doping of second metal prevented the usual particle agglomeration. High dispersion of binary nanocomposites on the surface of mesoporous SBA-15 has been achieved successfully through in-situ precipitation – deposition method.

$\text{Mn}_2\text{O}_3\text{-SnO}_2$ nanocomposites were prepared successfully by a facile and green co-precipitation method, wherein, Instead of using organic mild base like hexamethylenetetramine highly diluted ammonia solution is used. Both manganese and tin salts are dissolved in water rather than using harmful organic solvents in the preparation of nanoparticles. No capping agents or stabilizing agents are used for the preparation of nanocomposites. To prevent the agglomeration of nanoparticles a second metal oxide is used successfully. A highly quality hexagonally ordered mesoporous silica SBA-15 has been prepared successfully. The nanocomposites of $\text{Mn}_2\text{O}_3\text{-SnO}_2$ were prepared by GSA method has been carefully dispersed on the pore walls of silica SBA-15 by precipitation-deposition technique. The structural and textural properties of Nano composites and the final $\text{Mn}_2\text{O}_3\text{-SnO}_2\text{-SBA-15}$ mesonano composite materials were confirmed by different characterization techniques like BET surface areas, XRD and SEM

5. References:

- [1] (a) A. sayari, *Chem. Mater.* 8 (1996) 1840, (b) A. Corma, *Chem. Rev.* 97 (1997) 2373, (c) J.Y. Ying, C.P. Mehnert, M.S. Wong, *Angew. Chem.Int.Ed.* 38 (1999) 56, (d) A. Hagfeldt, M. Gratzel, *Acc. Chem. Res.* 33 (2000) 269, (e) Y.Tao, H. Kanoh, L.Abrams, K.Kaneko, *Chem. Rev.* 106 (2006) 896 (f) J.A.Melero, R. Van Grieken, G. Morales, *Chem. Rev.* 106 (2006) 3790 (g) M. Valler-Reg, *Chem. Eur. J.* 12 (2006) 5934.
- [2] (a) D.Wang, R.A.Caruso, F.Caruso, *Chem. Mater.* 13 (2001) 364, (b) A.Imhof, G.J.Pine, *Adv.Mater.* 11 (1999) 311
- [3] R.D.Muller, *Science* 286 (1999) 241
- [4] (a) S.Shimuzu, H. Hamada, *Adv.Mater.* 1 (2000) 1332, (b) Y.Lee, J.S.Lee, Y.S. Park, K.B. Yoon, *Adv. Mater.* 13 (2001) 1259, (c) S. Mintova, T. Bein, *Adv. Mater.* 13 (2001) 1880
- [5] (a) J.-L. Shi, Hua, L.-X Zhang, *J. Mater. Chem.* 14 (2004) 795, (b) K.Yamamoto, Y. Sunagawa, H. Takahashi, A. Muramatsu, *Chem. Commun.* (2005) 348, (c) P. Han, X. Wang, X Qiu, X. Ji, L Gao, *J. Mol. Catal. A: Chem.* 272 (2007) 136
- [6] (a) C.-M Yang, P.-H. Liu, Y.-F.Ho, C.-Y. Chiu, K.-J. Chao, *Chem. Mater.* 15 (2003) 275, (b) L. Li, J.-L. Shi, L.-X. Zhang, L.-M. Xiong, J.-N. Yan, *Adv. Mater.* 16 (2004) 1079
- [7] (a). E.R.Leite, A. p. Maciel, I. T. Weber, P. N. Liaboa-Filho, E. Longo, C. O. Paiva-Santos, A.V.C. Andrade, C. A. Pakoscimas, Y. Maniette and W.H. Shreiner, *Adv. Matter.* 14 (2002) 905.(b). E.R.Leite, I. T. Weber, E. Longo, J.A. Varela, *Adv. Mater.* 12 (2000) 965.
- [8] D.Zhao, Q.Hua, J.Feng, B.F.Chmelka, G.D.Stucky, *J.Am.Chem.Soc.* 120(1998)6024

